Ultrasonic Guided Wave Testing with Dragonfly®

Emil Garnell, R&D engineer at Wormsensing
www.wormsensing. com | contact@wormsensing.com
Grenoble, France - 2024/08/01

Abstract

Ultrasonic Guided Wave (UGW) testing is emerging as one of the most efficient techniques for detecting, locating, and evaluating damage in structures. It is based on measuring the propagation of high-frequency waves between an array of piezoelectric transducers installed on the structure. However, its widespread use has been limited by the difficulty of integrating piezoelectric sensors into real structures due to the brittleness of standard transducers. Dragonfly®, the piezoelectric strain sensor developed by Wormsensing, exhibits high sensitivity and wide bandwidth, yet is thin and flexible. To demonstrate its potential for UGW testing, an aluminum plate is instrumented with an array of Dragonfly® sensors. An artificial damage to the plate is detected and localized using the RAPID algorithm.

Key Words
UGW testing, RAPID algorithm, piezoelectric sensor, SHM

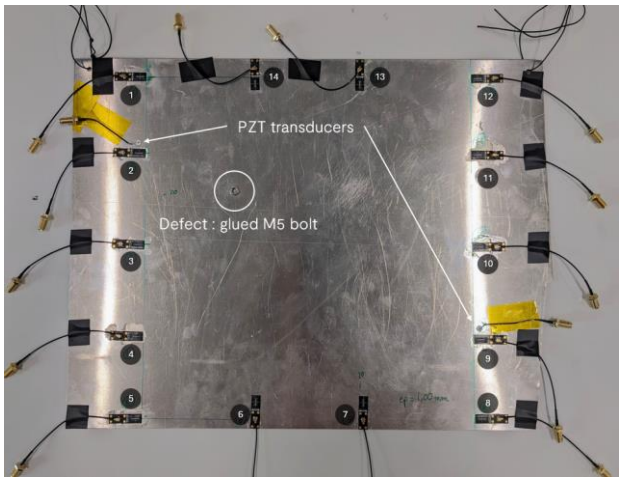

Figure 1 : Picture of the studied aluminum plate, with the 14 Dragonfly® sensors glued all around the plate border. Two additional PZT transducers are placed close to sensors 2 and 9 for comparison purposes. A defect is simulated by gluing an M5 bolt to the plate at the indicated location.

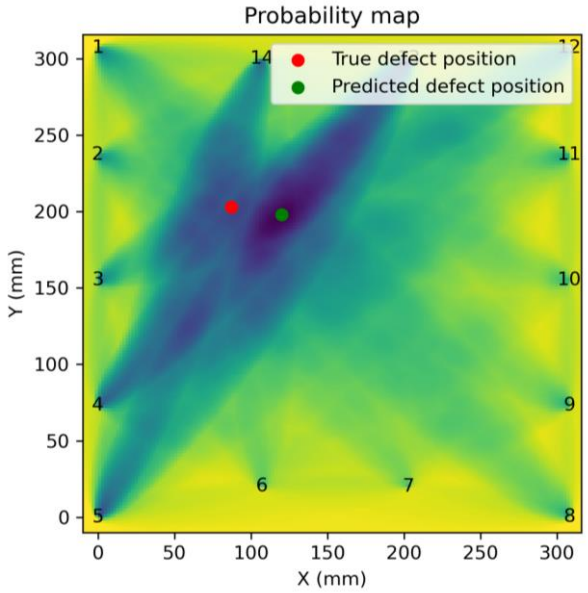

Figure 2 : Results of the RAPID algorithm, showing the probability of the presence of a defect at all positions. The red dot represents the true defect position, and the green dot is the predicted defect position, obtained as the maximum amplitude of the probability map. The numbers identify the transducers of the array.

1 Introduction

Among Structural Health Monitoring (SHM) technologies, Ultrasonic Guided Wave (UGW) testing arises as one of the most promising techniques to detect and localize defects on structures, such as cracks, impact damages, and corrosion. It has been historically widely used for the monitoring of pipes, where the propagation of ultrasonic waves is easily interpreted [1].

More recently UGW has gained interest in the monitoring of plate-like structures, like for example aircraft fuselages [2]. The principle is to place an array of piezoelectric transducers around (or in) the area to be monitored, and to alternatively emit a burst "of ultrasonic waves" on each transducer and measure its propagation to the other transducers of the array. The typical frequencies of interest lie between 10kHz and a few MHz.

Several post-processing techniques exist for analyzing the measured signals and producing a map of probable damages, some of which require a baseline measurement without defect, and then compare the measurements in the actual state to this baseline. Deviations from the baseline may be linked to defects on the plate. These techniques suffer from their sensitivity to environmental conditions. For example, a change in temperature alters the wave velocity in the plate, creating differences between the current measurements and the baseline that are not caused by defects in the structure being tested. However, several solutions have been developed to compensate the influence of environmental conditions [3].

Another category of signal processing techniques consists of baseline-free methods that do not require measurement in a defect-free state. These methods are based on modeling the propagation of waves in the structure under inspection. They are more difficult to apply to complex structures that are not simple plates, but allow the detection of defects that existed before the transducer array was installed [4].

The pre-requisite for successful deployment of UGW testing, no matter which post-processing algorithms are used, is the integration of sensitive and robust piezoelectric transducers in the studied structure. The most commonly used sensors are Lead zirconate titanate (PZT) disks, which provide a high sensitivity at a reduced cost. However, they are very brittle and are hard to integrate in a reliable manner in industrial structures.

In this article, we study the use of Dragonfly® piezoelectric sensors, manufactured by Wormsensing for UGW testing. These sensors are thin, flat and flexible, and thus straightforward to integrate in any object. Moreover, Wormsensing has the ability to design and manufacture custom flexible PCBs which may integrate several piezoelectric elements, which considerably reduces the installation effort and increases the reliability of the sensor array.

To demonstrate the relevance of Dragonfly® for UGW testing, an experimental study is conducted on an aluminum plate, where an artificial defect is detected and localized using a standard UWG processing technique: the RAPID algorithm [5]. Dragonfly® is also compared to standard PZT sensors in terms of sensitivity, frequency response, and ease of integration.

2 Setup

2.1 Studied plate

A 1mm-thick aluminum plate of dimensions 400*320mm approximately is instrumented with 14 Dragonfly® sensors, regularly spaced on the plate border, see Figure 1. The plate is made of standard aluminum, whose longitudinal wave velocity is around 6420m/s and shear wave velocity around 3040m/s. The dispersion curve of the Lamb waves propagating in the plate is computed using the Python Lamb-Wave-Dispersion package [6], and the group velocity of the different modes is plotted in Figure 3.

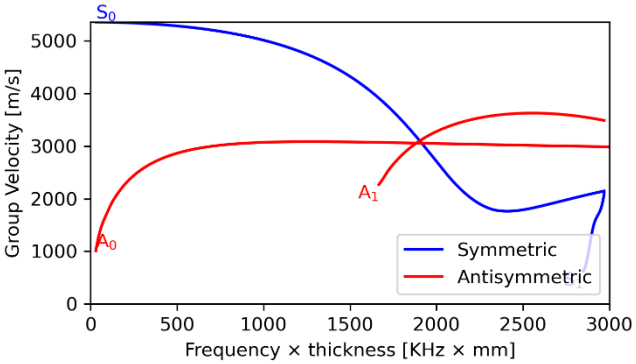

Figure 3 : Group velocity of lamb waves in the aluminum plate, for the first 2 symmetric and antisymmetric modes.

The excitation frequency is set to 100kHz, and at this frequency only two modes propagate: the A0 and the S0 modes. The S0 mode is much faster than the A0 mode.

2.2 Measurement setup

The excitation frequency is chosen at 100kHz, and the excitation signal consists of a burst of 10 periods of sine wave, modulated by a Hanning window. The excitation signal is plotted in Figure 4 together with the response of transducer 3 when the burst is sent to transducer 8.

The burst is generated by a Keysight 33500B waveform generator. The target amplitude of the burst is set to 10V peak-to-peak which is the maximum amplitude which can be generated by the waveform generator. It is worth noticing that the excitation amplitude is at least one order of magnitude below the typical excitation levels generally used for UGW testing. This may result in lower signal to noise ratio in the current measurements than in standard UGW setups.

The generated signal and the transducer responses are recorded by a Spectrum M4i.2234-x8 acquisition card, sampling at 2MHz. This acquisition card has a limited SNR of 45dB approximately. The transducer signals are pre-amplified before entering the Spectrum card by a home-made voltage amplifier with a gain of x48 (34dB), based on an OPA827 operational amplifier. The amplitude of signals plotted in Figure 4 is the amplitude measured by the acquisition card, and thus after the amplifiers.

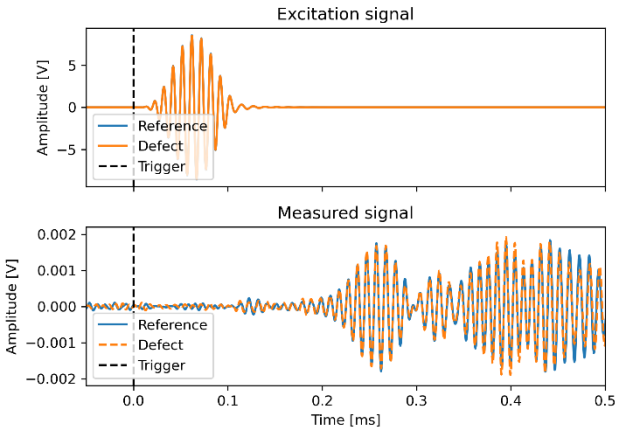

Figure 4 : (a) Excitation signal, consisting of 10 periods of a sine wave at 100kHz, modulated by a Hanning window. (b) Response of transducer 3 when the burst is played on transducer 8, during the first 0.5ms after the emission. The blue curves correspond to the reference state, and the orange ones to the signals measured with the defect (the M5 bolt glued on the plate).

All possible source-receiver paths are measured, by groups of two: one transducer is connected to the signal generator, and two others to the acquisition card. A measurement is performed, and the two next transducers are connected to the acquisition card. Once all transducers have been measured as receivers for the selected source transducer, the procedure is repeated with all other transducers as sources. In total 14*13=182 source-receiver paths are measured.

3 Signal processing

The Reconstruction Algorithm for Probabilistic Inspection of Damage (RAPID) is used to process the measured signals and localize the defect [5], [7].

The first step is to crop the signals to the region of interest, to keep the first burst cycles after the arrival of the desired mode. The theoretical group velocity is used to compute the arrival time of the burst for a given source-receiver pair, which is shown in Figure 5.

On most measurements the fastest mode, the symmetrical S0 mode is not visible in the measured signals. There may be two reasons for this observation: either the sensors themselves do not couple well to this mode, or the noise floor is too high to see this mode in the measured signals.

Thus, only the A0 mode (which corresponds to bending waves at low frequencies) will be considered during the analysis, and all measured signals are cropped to a window starting at the arrival time of the A0 mode and lasting 0.1ms, which corresponds to the length of the excitation burst. The selected part of the signal is highlighted in Figure 5.

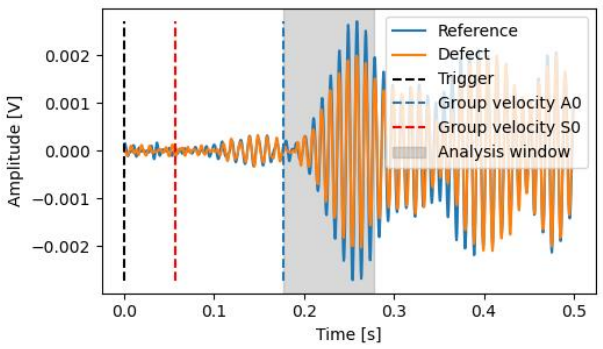

Figure 5 : Measured baseline and defect signals when the burst is played on transducer 3 and measured by transducer 12. The part of the signal which will be used in the rest of the analysis is highlighted in grey.

To build a metric representing the difference between the signals measured before and after the creation of a defect on the plate, the Signal Difference Coefficient (SDC) is used. It is defined as follows:

$$SDC = 1 - \rho$$

Where:

$$\rho = \frac{\mathrm{cov}(s_j, s_k)}{\sigma_j \sigma_k}$$

Where the covariance between the signal measured by sensor j (s_j) and by sensor k (s_k) is defined as:

$$\mathrm{cov}(s_j, s_k) = \frac{\sum_i^N (s_j(t_i) - \bar{s_j})(s_k(t_i) - \bar{s_k})}{N}$$

and where σ_j and σ_k are the standard deviations of the signals s_j and s_k.

The SDC is computed for all paths, and the SDC matrix representing the SDC between the reference and defect state for all sensors pairs is plotted in Figure 6.

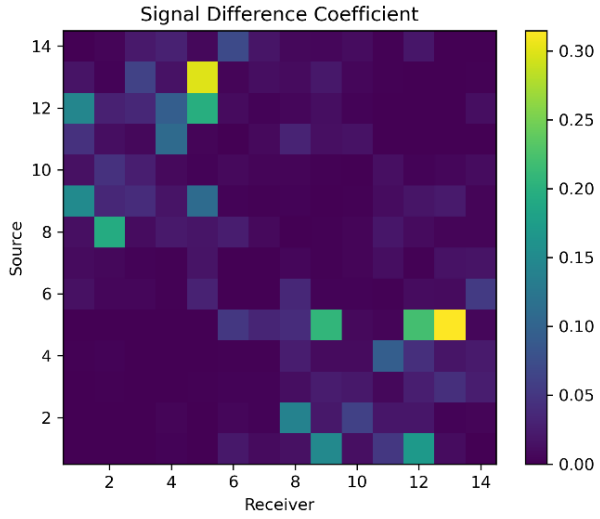

Figure 6 : SDC matrix, representing the SDC for all sensors pairs.

Figure 6 shows that the SDC matrix is almost symmetrical, which is expected because of the reciprocity principle (if a defect lies on the path between two sensors it should affect in the same manner the waves propagating in one direction or in the other). Here, the path which is the most affected by the defect is between sensors 5 and 13, which is coherent with the position of the defect.

4 Results

The defect probability map is built using the RAPID algorithm, by superimposing ellipses linking each source-receiver pair, whose density is proportional to the SDC coefficient of this pair (see [7] for the computational details).

The result is plotted in Figure 2. The scaling parameter β which governs the ellipse width in the RAPID algorithm was set to 1.015.

Figure 2 shows that the RAPID algorithm run with the data measured by the array of Dragonfly® sensors succeeds in detecting and localizing the defect. The distance between the true and the predicted defects is 34mm, which is in the standard order of magnitude of standard localization errors for low frequency UGW testing. Moving up to higher frequencies may help improving the spatial resolution. Also, more involved thresholding techniques may be used to increase the localization accuracy [7].

Of course, as the signals measured by the array of Dragonfly® sensors exhibit a good SNR, any other signal processing technique which has been developed in the field of UGW testing should work as well. We only tested the RAPID algorithm here as it seems to be one of the most widely used ones.

5 Comparison with standard PZT transducers

The sections above showed that the array of Dragonfly® sensors can perform UGW testing using standard processing algorithms, like RAPID. We will now analyze in more detail the major differences between the most used transducers for UGW testing on the market, namely PZT disks and Dragonfly® sensors, in terms of sensitivity, frequency response and integration in real products. A commercial Acoustic Emission (AE) transducer is also included in the benchmark (Vallen Systems VS150-M). The frequency response of this sensor is characterized by a peak at 150kHz.

Dragonfly® is compared to standard PZT sensors available on the market, made of PZT-5H piezoelectric material, with a diameter of 5mm and a thickness of 0.3mm. Two of these sensors are glued using cyanoacrylate glue to the aluminum plate as shown in

Figure 1. A close view of a PZT transducer and of the AE sensor is shown in Figure 7.

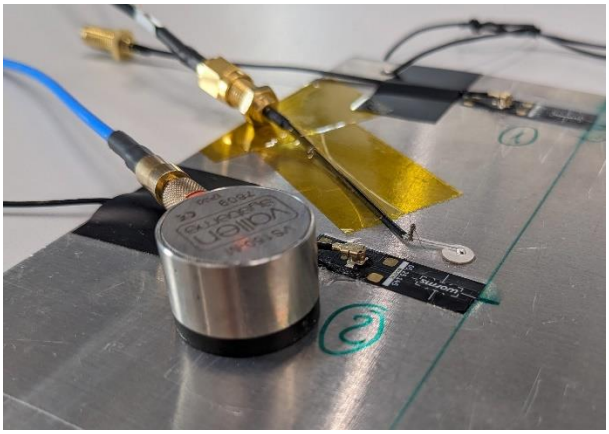

Figure 7 : close view of Dragonfly® number 2, of the PZT disk and of the commercial AE sensor glued close by.

5.1 Sensitivity as emitters

To assess the sensitivity of Dragonfly® vs. the PZT sensor as emitter, a frequency sweep from 100Hz to 2MHz is sent successively by the Dragonfly® number 9 and by the PZT disk number 9. The transmitted waves are measured by Dragonfly® number 2 on the other side of the plate. The response of sensor 2 to the two sweeps is plotted in Figure 8.

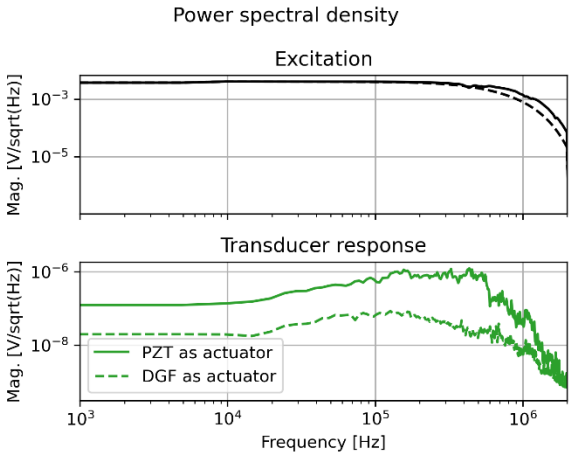

Figure 8 : Response of Dragonfly® number 2 to a sweep sent to the PZT disk at position 9 and to Dragonfly® at position 9.

The linear sweep is designed to have a constant amplitude from 100Hz to 2MHz, and thus a flat PSD in this frequency range. Figure 8 shows that the excitation voltage applied to the transducer decreases at high frequencies, most certainly due to limitations of the signal generator which has been used, which is not able to provide sufficient current to drive the capacitive loads at high frequencies. All the measured responses thus also decrease above 500kHz, because of the limitations of the signal generator.

Figure 8 shows that when the same excitation signal (a sweep at +- 10V from 100Hz to 2MHz) is sent successively by the PZT actuator and by Dragonfly®, the response of another Dragonfly® located on the other side of the plate is approximately 10 to 50 times higher when the sweep is played on the PZT disk, meaning that for the same excitation signal more energy is put into the plate by the PZT disk. This is quite expected, and directly related to the amount of piezo material contained in both sensors:

- The PZT disk contains approximately 2mm^3 piezo material.
- The active area of Dragonfly is less than 10µm-thick, and its planar dimensions are 1.5*5mm, resulting in a volume around 0.08mm^3.

The PZT disk contains approximately 30 times more piezoelectric material than Dragonfly®, which may explain the sensitivity difference.

5.2 Sensitivity as receivers

To test the sensitivity as a sensor, the same setup is used but this time to compare the signals measured by the three tested transducers (AE, PZT and Dragonfly® - DGF). The sweep between 100Hz and 2MHz is sent to Dragonfly® number 9 and recorded by the three sensors located at position 2 and shown in Figure 7. The measured time signals are plotted in Figure 9.

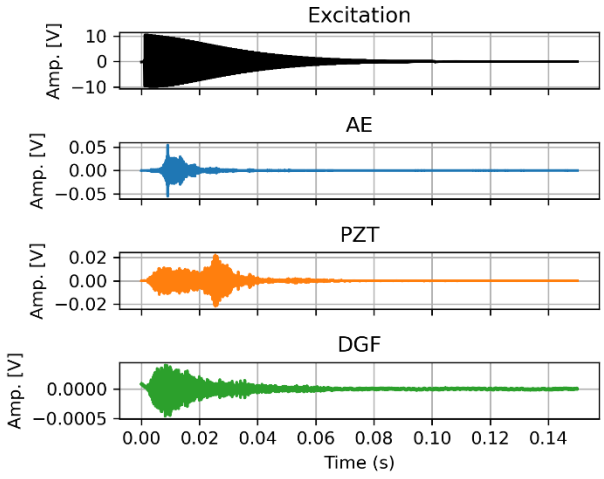

Figure 9 : Excitation signal and transducer responses. The signal is sent by Dragonfly® number 9 and recorded by the transducers at location number 2.

Figure 9 shows that the amplitude of the measured signal is higher for the AE sensor and for the PZT disk than for Dragonfly®. This is again expected as the piezoelectric element of Dragonfly® is much thinner than the other sensors, and thus generates a lower voltage. Moreover, a clear peak around 1ms

can be seen in the response of the AE sensor, an another one at 2.5ms in the signal of the PZT disk, revealing resonance phenomena. To investigate this further, the PSDs of the recorded signals are plotted in Figure 10.

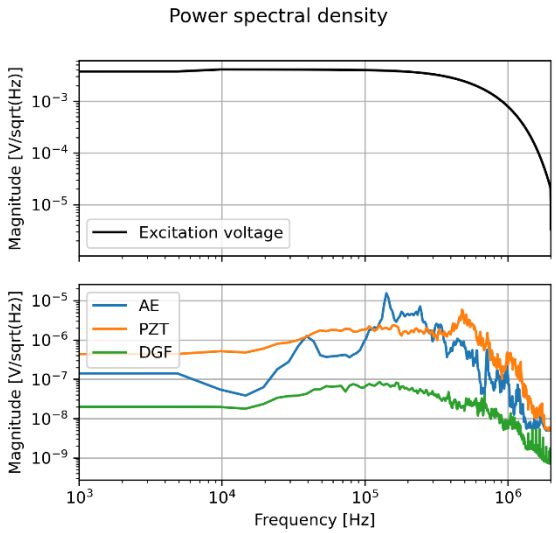

Figure 10 : Power Spectrum Density of the excitation signal and of the transducer responses. The signal is sent to Dragonfly® number 9 and recorded by the transducers at location number 2.

Figure 10 shows that the AE sensor clearly exhibits a resonance at 150kHz, as specified in its datasheet. The PZT disk also resonates at 500kHz. On the other hand, Dragonfly has a much flatter frequency response, with no visible resonances in the studied frequency range. The sensitivity of Dragonfly seems to be around 50 times lower than the PZT disk and the AE sensor in these testing conditions.

5.3 Integration issues

Some of the main limitations for the deployment of UGW testing in real conditions come from integration issues. To be able to detect and localize a defect in an area, many sensors are usually required. The sensor array must be easy to integrate, lightweight, flat and robust: sensor damage of drift may be hard to distinguish from true defects.

The most used sensors for UGW testing are PZT disks, because of their wide availability, limited cost, and high sensitivity. However, they suffer from their brittleness, which makes them hard to integrate with a high success rate. Also, the cabling is often the heaviest part of the system, if each sensor has its own cable.

To try to make PZT sensor arrays easier to integrate, some research teams are working on flexible PCBs integrating several sensors and multiplexing electronics reduce the cabling effort [8]. Sandwiching the PZT element between two layers of polymers makes it less brittle and easier to integrate without breaking it, but there are still issues with the gluing and its stability over time [9].

The piezoelectric element developed by Wormsensing is so thin that it is flexible by nature and can be glued on curved surfaces without breaking it (see Figure 11).

Figure 11 : Pictures of Dragonfly® glued on a 20mm radius cylinder.

Moreover, the manufacturing process makes this element fully compatible with standard pick-and-place tools commonly used in the electronics industry to assemble components on flexible PCBs. Thus, this element is a promising candidate for manufacturing robust UGW arrays, which are very thin, flexible, robust, and easy to manufacture (see Figure 12).

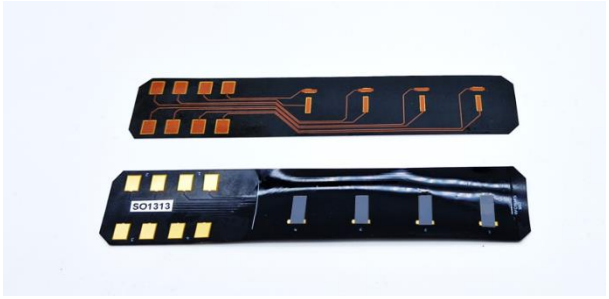

Figure 12 : Example of the integration of several piezoelectric elements manufactured by Wormsensing on a flexible PCB, to obtain a flexible sensor array.

6 Conclusions

To conclude, a typical Ultrasonic Guided Wave testing setup has been implemented on an aluminum plate using Dragonfly® piezoelectric transducers. The propagation of Lamb waves at 100kHz through the plate between all the transducer pairs has been measured, and the RAPID tomography algorithm has been used to detect and localize a defect simulated by an added bolt on the plate. The localization error is around 3cm on a 40cm wide plate.

Its sensitivity may be lower than conventional PZTs, but it is also much lighter and thinner and does not exhibit any resonance under 2MHz. Thanks to its flexibility, robustness, and easy integration into standard flexible PCBs, Dragonfly® appears to be a suitable candidate for UGW testing, as it helps solving deployment issues caused by the brittleness and bulkiness of standard PZT elements. Moreover, it is lead free which is a major argument today regarding the evolving environmental regulations.

References

[1] M. J. S. Lowe, D. N. Alleyne, and P. Cawley, "Defect detection in pipes using guided waves," *Ultrasonics*, vol. 36, no. 1, pp. 147–154, Feb. 1998, doi: 10.1016/S0041-624X(97)00038-3.

[2] P. Puthillath and J. L. Rose, "Ultrasonic guided wave inspection of a titanium repair patch bonded to an aluminum aircraft skin," *Int. J. Adhes. Adhes.*, vol. 30, no. 7, pp. 566–573, Oct. 2010, doi: 10.1016/j.ijadhadh.2010.05.008.

[3] Z. Dworakowski, L. Ambrozinski, and T. Stepinski, "Multi-stage temperature compensation method for Lamb wave measurements," *J. Sound Vib.*, vol. 382, pp. 328–339, Nov. 2016, doi: 10.1016/j.jsv.2016.06.038.

[4] Fei Yan, R. L. Royer, and J. L. Rose, "Ultrasonic Guided Wave Imaging Techniques in Structural Health Monitoring," *J. Intell. Mater. Syst. Struct.*, vol. 21, no. 3, pp. 377–384, Feb. 2010, doi: 10.1177/1045389X09356026.

[5] J. Hettler, M. Tabatabateipour, S. Delrue, and K. Van Den Abeele, "Application of a Probabilistic Algorithm for Ultrasonic Guided Wave Imaging of Carbon Composites," *Phys. Procedia*, vol. 70, pp. 664–667, 2015, doi: 10.1016/j.phpro.2015.08.072.

[6] F. Rotea, *franciscorotea/Lamb-Wave-Dispersion*. (Jun. 06, 2024). Python. Accessed: Jul. 10, 2024. [Online]. Available: https://github.com/franciscorotea/Lamb-Wave-Dispersion

[7] T. R. Hay, R. L. Royer, H. Gao, X. Zhao, and J. L. Rose, "A comparison of embedded sensor Lamb wave ultrasonic tomography approaches for material loss detection," *Smart Mater. Struct.*, vol. 15, no. 4, pp. 946–951, Aug. 2006, doi: 10.1088/0964-1726/15/4/007.

[8] D. Schmidt *et al.*, "Development of a Door Surround Structure with Integrated Structural Health Monitoring System," in *Smart Intelligent Aircraft Structures (SARISTU)*, P. C. Wölcken and M. Papadopoulos, Eds., Cham: Springer International Publishing, 2016, pp. 935–945. doi: 10.1007/978-3-319-22413-8_51.

[9] S. Galiana, M. Moradi, P. Wierach, and D. Zarouchas, "Innovative welding integration of acousto-ultrasonic composite transducers onto thermoplastic composite structures," *Struct. Health Monit.*, p. 14759217241247766, Apr. 2024, doi: 10.1177/14759217241247766.